Pergamon

J. Biomechanics Vol. 28, No. 4, pp. 423–437, 1995

0021-9290/95 $9.50 + .00

0021-9290(94)00080-8

ACCURACY ASSESSMENT OF METHODS FOR DETERMINING HIP MOVEMENT IN SEATED CYCLING

R. R. Neptune and M. L. Hull

Department of Mechanical Engineering, University of California, Davis, CA 95616, U.S.A

Abstract—The goal of this research was to examine the accuracy of three methods used to indicate the hip joint center (HJC) in seated steady-state cycling. Two of the methods have been used in previous studies of cycling biomechanics and included tracking a marker placed over the superior aspect of the greater trochanter, a location that estimates the center of rotation of the hip joint, and assuming that the hip is fixed. The third method was new and utilized an anthropometric relationship to determine the hip joint location from a marker placed over the anterior–superior iliac spine. To perform a comparative analysis of errors inherent in the three methods, a standard method which located the true hip joint center was developed. The standard method involved establishing a pelvis-fixed coordinate system using a triad of video markers attached to an intracortical pin. Three-dimensional motion analysis quantified the true hip joint center position coordinates.

To provide data for the comparative analysis, the intracortical pin was anchored to a single subject who pedaled at nine cadence–workrate combinations while data for all four methods were simultaneously recorded. At all cadence–workrate combinations the new method was more accurate than the trochanter method with movement errors lower by a factor of 2 in the vertical direction and a factor of 3 in the horizontal direction. Relative to the errors introduced by the fixed hip assumption, the new method was also generally more accurate by at least a factor of 2 in the horizontal direction and had comparable accuracy in the vertical direction. For computed kinetic quantities, the new method most accurately indicated hip joint force power but the fixed hip method most accurately indicated the work produced by the hip joint force over the crank cycle.

INTRODUCTION

Studies of cycling which compute kinetic biomechanical quantities (e.g. intersegmental loads) through inverse dynamics generally model the rider–bicycle system as a planar five-bar linkage fixed at the crank axis (e.g. Hull and Jorge, 1985). The links consist of the bicycle crank, thigh, shank, foot and segment joining the hip to the crank spindle. Fundamental to solving the inverse dynamics problem is the determination of the lower extremity kinematics. One method is to derive the kinematics through analytical equations based on geometry and the kinematic data of the pedal and crank arm (e. g. Hull and Jorge, 1985). A second method is to use video analysis to record the time histories of reflective skin markers placed over the joint centers (Gregor *et al.*, 1991). The video image is then digitized to record the segment motion histories which are differentiated with respect to time to obtain segment velocities and accelerations.

Whether the researcher uses either the analytical derivation or the video based method to compute the lower extremity kinematics, the accuracy of the data ultimately affects biomechanical quantities computed by the inverse dynamics solution. Errors in joint position, velocity, and acceleration directly affect computed joint moments, power, and work, the biomechanical quantities important to studies of cycling biomechanics.

Fundamental to the accuracy of the kinematic data particularly of the thigh segment is the methodology used to locate the hip joint center (HJC). The most common method utilizes high speed cameras to record the time history of a reflective skin marker placed over the superior aspect of the trochanter (e.g. Gregor *et al.*, 1985; van Ingen Schenau *et al.*, 1990). Although this simple technique is appealing to experimentalists, soft tissue movement and marker misalignment can introduce errors in joint coordinates which alter computed kinematics hence introducing errors into biomechanical quantities determined through kinetic analysis.

Another method is to assume that the HJC remains stationary throughout the crank cycle (e.g. Hull and Gonzalez, 1990). An estimation of the HJC is made by taking anthropometric measurements of the superior aspect of the greater trochanter relative to a reference coordinate system. If hip motion does exist however, then errors can be introduced in computed biomechanical quantities by using the fixed hip assumption. This is especially true for both power and work associated with the joint reaction force applied to the thigh by the pelvis. By assigning fixed coordinates to the HJC, both the power and work are set to zero.

Recognizing the potential sources of error using either the trochanter or fixed hip methods, a new method was developed which was hypothesized to be

Received in final form 18 *February* 1994.

Address correspondence to: Prof. M. L. Hull, Dept Mechanical Engineering, University of California, Davis, CA 95616, U. S. A.

more accurate in tracking the HJC. The new method determined the position of the HJC from video data of the anterior–superior iliac spine. Thus one objective of the work reported in this paper was to test the hypothesis that the new method is more accurate. To address this objective, comparisons in both measured hip motion and computed biomechanical quantities were performed. Considering that cycling studies are performed at a variety of cadences and workrates, a second objective was to investigate errors associated with each method as a function of cadence and workrate. Specifically, the hypothesis that errors do not increase with pedaling rate and workrate was tested.

METHODS

One competitive male cyclist (age 45 yr, height 1.75 m, weight 73.5 kg), volunteered for participation in this study. Informed consent was obtained before the experiment. The subject rode a conventional racing bicycle mounted on a Velodyne cycling ergometer. The bicycle configuration was adjusted to match the prefered geometry of his own bike, so that seat and handlebar height were not controlled.

Hip joint kinematics were analyzed using four methods with necessary data recorded simultaneously using video analysis. A standard method (STD) was developed to provide a platform for comparison between the fixed hip, trochanter, and new methods. Using standard surgical procedures, the skin over the right iliac crest was cleaned using betadine. Lidocaine (2%) was used to anesthetize the skin, subcutaneous tissue, periosteum, and bone. A 3 mm self-tapping intracortical pin was threaded 2 cm into the lateral iliac crest using a surgical drill. No incision was necessary due to the thin soft tissue layer in this region. The subject reported mild discomfort during the procedure which lasted five minutes. A triad of three reflective spheres (2.5 cm diameter) located 17.0 cm equidistant apart was attached to the pin 6.5 cm from the insertion point (Fig. 1). Once the desired orientation of the triad was established, set screws were tightened and sealed with an epoxy resin. Two X-rays were taken perpendicular to the sagittal (lateral view) and frontal (anterior–posterior view) planes to establish a vector $\mathbf{V}^{T_pH}$ from the centroid of the pin marker T_p to the hip joint center H (Fig. 2) in the laboratory coordinate system (X, Y, Z). The HJC was defined as the center of the spherical femoral head. The orthogonality of the X-ray views was attained through an iterative process. X-ray calibration was performed by placing a known calibration device in both the lateral and anterior–posterior views to conduct a direct linear transformation on the vector measurements.

Three-dimensional motions of the triad markers were recorded at 60 Hz using three cameras positioned perpendicular to the frontal and sagittal planes and one oriented at 45°. The video data were filtered using a fourth-order zero phase shift Butterworth low pass filter with a cutoff frequency of 9 Hz. Data were calibrated and analyzed to reconstruct the time histories of the markers.

The location of the HJC in the laboratory coordinate system was computed in several steps. First the vector $\mathbf{V}^{T_pH}$ measured from the X-ray views in the laboratory coordinate system was transformed into the triad fixed coordinate system (x, y, z) (Fig. 2). This transformation was accomplished through video analysis of the triad markers in both the position and orientation of the triad in the X-ray views. Next, the video data recorded while the subject was cycling were analyzed to transform the vector $\mathbf{V}^{T_pH}$ back into the laboratory coordinate system. These transformations were necessary because the vector $\mathbf{V}^{T_pH}$ is always fixed in the triad coordinate system but moves relative to the laboratory coordinate system when the subject cycles. Finally, the vector $\mathbf{V}^{T_pH}$ was added to $\mathbf{V}^{L,T_p}$ to locate the HJC. The mathematicl details of the vector analysis are given in the Appendix. A time history of the three-dimensional HJC coordinates was produced by computing the vector addition as a function of time from the recorded video data. These three-dimensional coordinates were then projected into the sagittal plane for comparison with the other methods.

The trochanter method (TRO) used a spherical marker placed over the superior aspect of the greater trochanter and assumed this to be the HJC. The video data were processed to produce a time history of the HJC horizontal and vertical components.

The new method (ASIS) determined the position of the HJC from a video marker placed over the anterior–superior iliac spine. A vector of fixed magnitude and orientation in the sagittal plane was established by computing the vector between the average anterior–superior iliac spine and trochanter coordinates. This vector was attached to the anterior–superior iliac spine to represent the center of the femoral head simulating the HJC. This method assumes that there is no rotation of the pelvis in the sagittal plane.

The fixed hip method (FIX) assumed that the HJC was fixed throughout the motion cycle. The HJC position was located by external anthropometric measurements from the laboratory coordinate system origin L_C to the superior aspect of the greater trochanter. After a warm-up period this measurement was made while the cyclist remained stationary with the crank arms positioned in a reference horizontal position. This position assumed the superior aspect of the greater trochanter to be located in the neutral position.

The assessment of errors associated with each of these methods consisted of a direct comparison of HJC position with the STD method, and the effect that any differences have on hip joint moment and power computations.

To compute the biomechanical quantities, the rider was modeled as a five-bar linkage in plane motion. The equations of motion for each link were solved using inverse dynamics, starting with the foot and

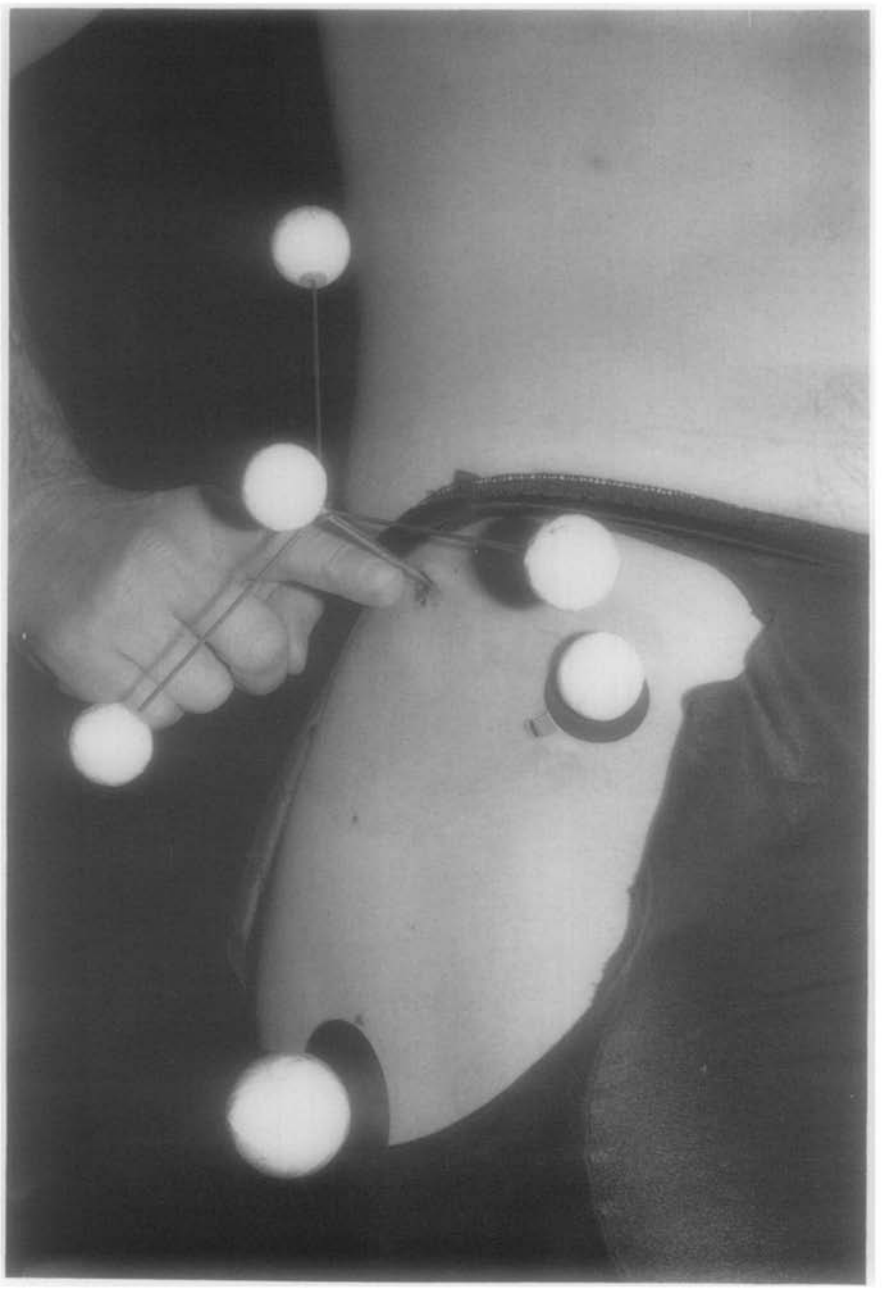

Fig. 1. Triad of video markers attached to intracortical pin inserted in the iliac spine. Additional spherical video markers are placed over the anterior superior iliac spine (ASIS) and the superior aspect of the greater trochanter.

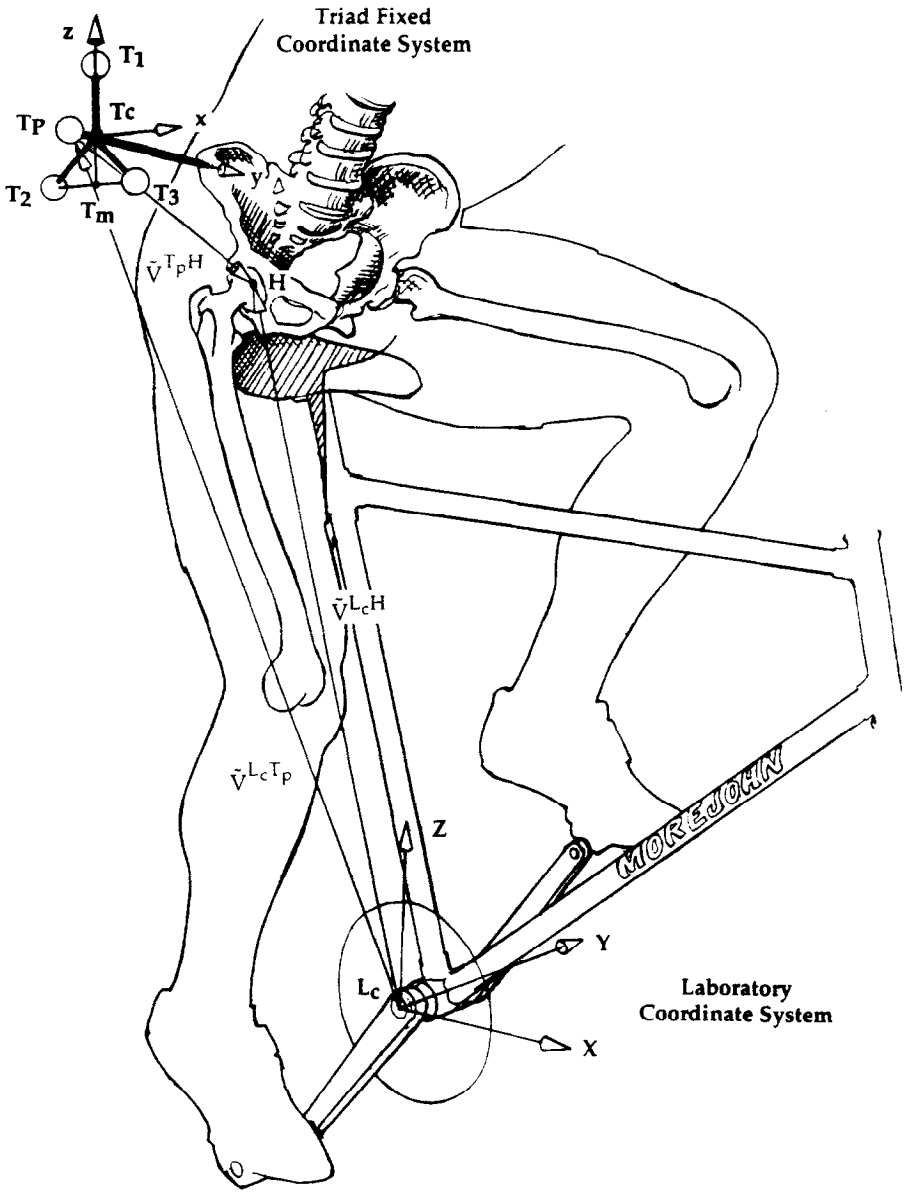

Fig. 2. Laboratory and triad fixed coordinate systems location and orientation. The origin of the triad coordinate system was located at the triad center T_c. The directions of the triad axes were determined by the triad markers. The X-axis was directed anteriorly parallel to the line joining markers T_2 and T_3, the Y-axis medially along the axis of the pin, and the Z-axis superiorly along the line joining points T_m and marker T_1. The hip joint center is located relative to the reference coordinate system by vector addition: $\mathbf{V}^{L_cH} = \mathbf{V}^{L_cT_p} + \mathbf{V}^{T_pH_n}$.

proceeding through each link to the hip. To provide the kinematic data, reflective markers placed over the right lateral epicondyle, lateral malleolus, pedal spindle, and crank spindle were videotaped simultaneously with the various hip markers at 60 Hz. The video data were filtered using a fourth-order zero phase shift Butterworth low pass filter with a cutoff frequency of 9 Hz. All derivatives to determine coordinate velocity and acceleration were calculated by fitting a quintic spline to the position data and differentiating the resulting equations.

Collected simultaneously with the kinematic data were pedal force profiles. To acquire these data, a pedal dynamometer similar to that described by Newmiller *et al.* (1988) was used. The dynamometer was modified to allow subjects to wear conventional clip-in cycling shoes. Weight was added to the opposite pedal to balance the inertial characteristics of the pedals. The pedal force data were filtered using a fourth-order zero phase shift Butterworth low pass filter with a cutoff frequency of 20 Hz. The filtered pedal force and encoder data were linearly interpolated to correspond in time with the video coordinate data.

The protocol consisted of a 10 min warm-up period at a workrate of 120 W at 90 rpm. To evaluate the

sensitivity of errors to both workrate and pedaling rate, the subject cycled at power levels of 150, 225 and 300 W and pedaling rates of 60, 90, and 120 rpm. These values were chosen to encompass the lower and upper ranges of typical cycling exercise. The workrate level was controlled by the Velodyne while the pedaling rate was controlled by the subject observing the Velodyne display screen. All three pedaling rates were performed at each of the three workrates yielding nine different combinations of pedaling rate and workrate. These combinations were randomly assigned using a random number table to avoid a systematic effect of fatigue. After a 2 min adaptation period, data collection was randomly initiated during the third minute for 10 s.

The comparative analysis was conducted in two steps at the 90 rpm and 225 W protocol. First, HJC total, bias and movement errors were computed as a function of crank angle for eight cycles collected within each 60 s collection period. For each of the eight cycles of data, the maximum, minimum, associated crank angles, and range of errors were averaged and tabulated for each combination of pedaling rate and workrate. The total error was computed by subtracting the HJC coordinates of the standard method from the other three methods. To assess the movement error, the bias error (i.e. average difference) associated with each method was subtracted from the total error data to quantify the difference in HJC movement from the standard.

The second part of the comparative analysis assessed differences in computed biomechanical quantities. Considering that inverse dynamic studies compute the intersegmental loads first at the foot, proceeding to the knee and then hip, only the biomechanical quantities of the hip will be altered noticeably by the kinematics of the HJC. Therefore only hip joint quantities were included in the comparative analysis. These quantities included the angular velocity of the thigh, the hip joint movement, the powers produced by both the hip joint force and moment, and the work done by the hip joint force. Because only one subject was tested, no statistical quantities were evaluated.

RESULTS

TRO had the greatest range of motion in both coordinate directions (Fig. 3) and was completely out of phase in the X-direction [Fig. 4(a) and (b)]. As a consequence, TRO had the greatest range of total error in both the X- and Z-directions at 2.7 and 3.6 cm, respectively (Fig. 5 and Table 1). ASIS had the lowest range of total error in the X-direction (0.5 cm) while FIX had the lowest range in the Z-direction (0.9 cm). Therefore, the hypothesis that ASIS was more accurate in indicating the true HJC position than both TRO and FIX was supported in the X-direction but not supported in the Z-direction.

Analysis of bias errors indicated that FIX located the true hip position on the average better than either of the video-based methods. The average X- and Z-coordinates of the HJC produced by STD were -24.9 and 72.0 cm, respectively. The corresponding average HJC coordinates of TRO and ASIS were -25.2, 69.7 and -25.2, 69.7 cm, respectively, suggesting that the average location of the trochanter marker was about 2.3 cm lower than the actual hip center. The measured coordinates locating the HJC in FIX were -25.0 and 71.0 cm which corresponded closely with STD.

Because ASIS produced similar movement in both magnitude and phase as STD whereas TRO yielded both magnitude and phase differences, TRO produced the greatest movement error in both coordinate

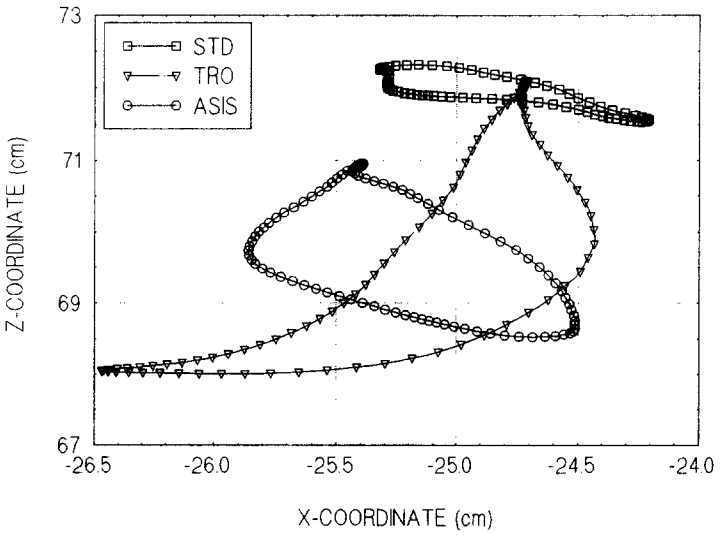

Fig. 3. Hip joint center absolute coordinate movement pattern over the full crank cycle (90 rpm, 225 W).

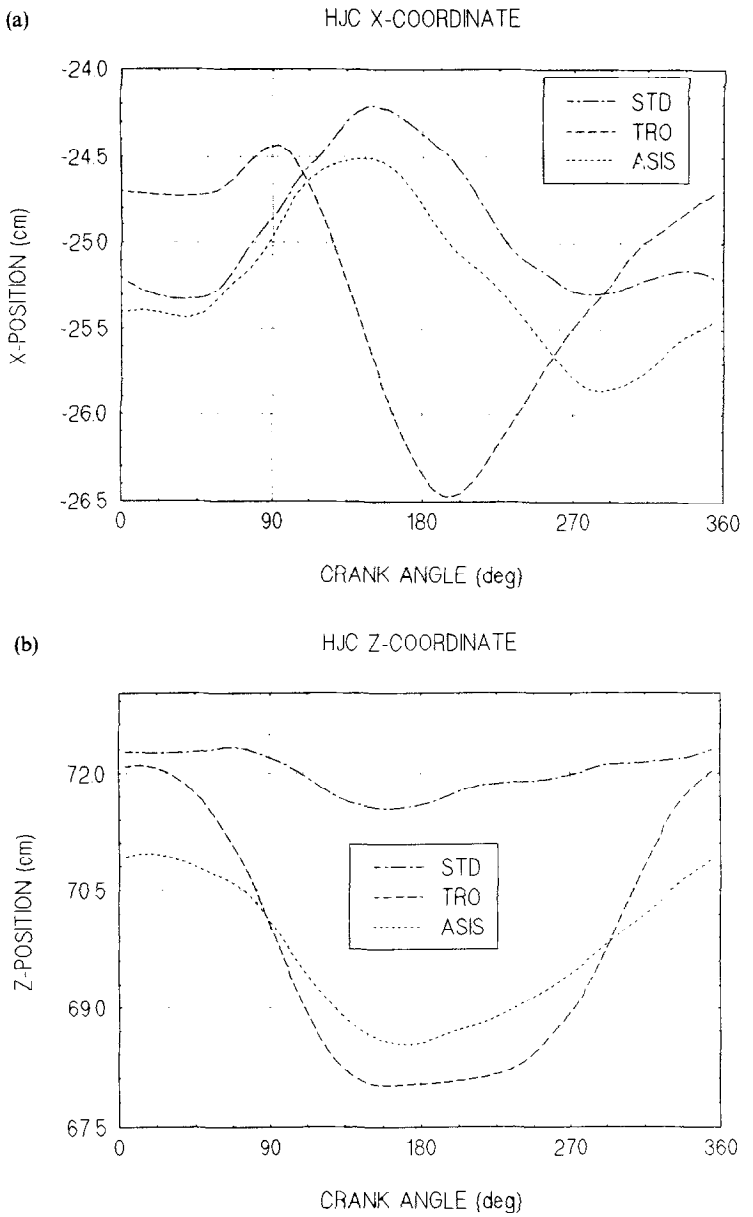

Fig. 4. Hip joint center X-coordinate (a) and Z-coordinate (b) position as a function of crank angle (90 rpm, 225 W). The top dead center position of the crank corresponds to an angle of 0° and the crank is horizontal and pointed forwards at 90°.

directions [Fig. 6(a) and (b)]. ASIS had the least movement error in the X-direction with a range of 0.5 cm while FIX had the least movement error in the Z-direction with a range of 0.9 cm (Table 2). These results are qualitatively similar to those for the total error.

In examining the effect of the methods on the computed biomechanical quantities, TRO underestimated the angular velocity peaks of the thigh (Fig. 7) whereas the moment developed at the hip as a function of crank angle showed only slight differences among the four methods (Fig. 8). Thus when these results were combined to generate the power developed by the hip joint moment, errors associated with TRO were the largest (Fig. 9). Considering the peak moment power generated, TRO produced the largest error at 4.9% (Table 3). ASIS and FIX had comparable errors at 3.0% and 3.2%, respectively. The largest relative errors occurred in the computation of the power produced by the hip joint force (Fig. 10). STD generated a peak power of 12.2 W compared to 43.2 W produced by TRO resulting in a 254% error (Table 4). This over estimate produced by TRO existed throughout the entire crank cycle and was quantified by the integral of the power curve resulting in the work produced by the hip joint force. TRO over estimated the hip joint force work by about 10 J or 384% as compared to the 2.5 J produced by STD (Table 5).

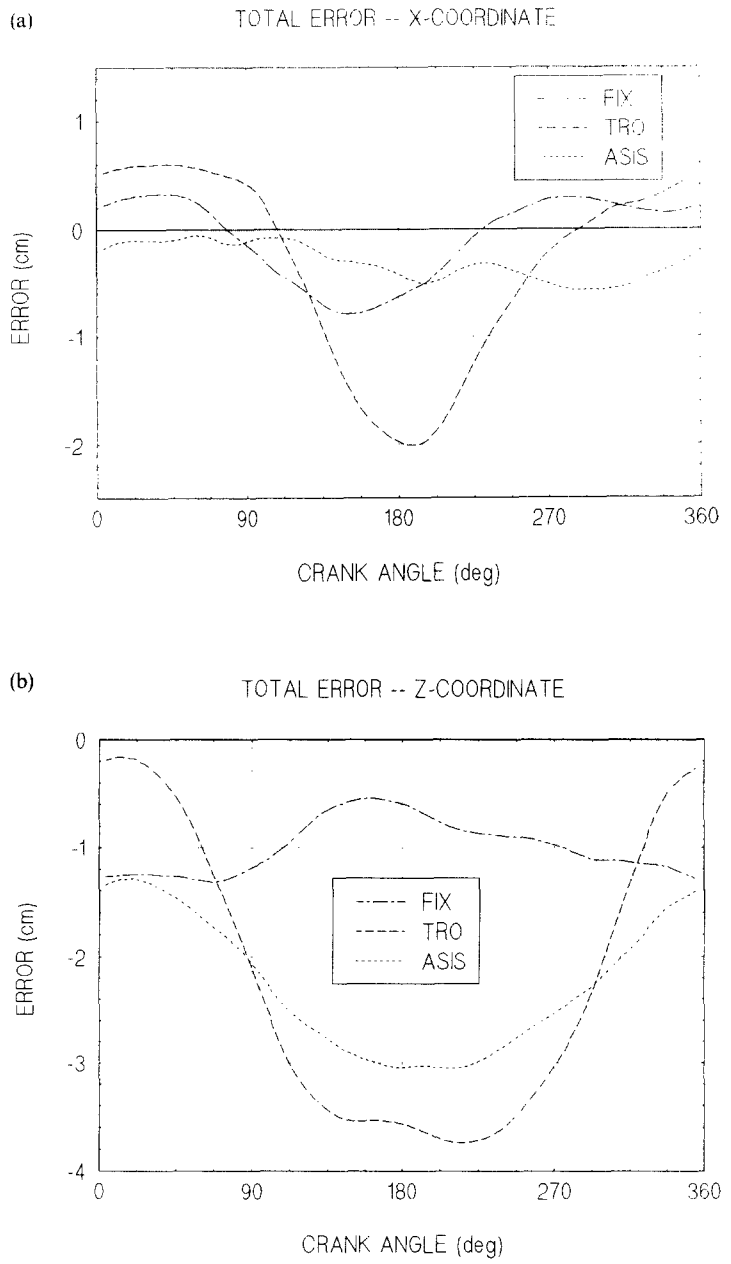

Fig. 5. Hip joint center X-coordinate (a) and Z-coordinate (b) total error as a function of crank angle (90 rpm, 225 W). The total error was defined as the difference in hip joint center coordinates from the standard method.

Table 1. Comparison of total error between methods (cm) (90 rpm, 225 W)

Method	Bias error	Standard deviation	Minimum error	Crank angle (deg)	Maximum error	Crank angle (deg)	Range of error
FIX_X	−0.1	0.4	0.0	79/230*	−0.8	149	1.3
FIX_Z	−1.0	0.3	−0.5	160	−1.4	68	0.9
TRO_X	−0.3	0.9	0.0	108/287*	−2.01	186	2.7
TRO_Z	−2.3	1.3	−0.1	7	−3.8	216	3.6
$ASIS_X$	−0.3	0.2	−0.05	64	−0.6	294	0.5
$ASIS_Z$	−2.3	0.6	−1.3	11	−3.1	195	1.9

* Minimum error occurs at two points during the crank cycle.

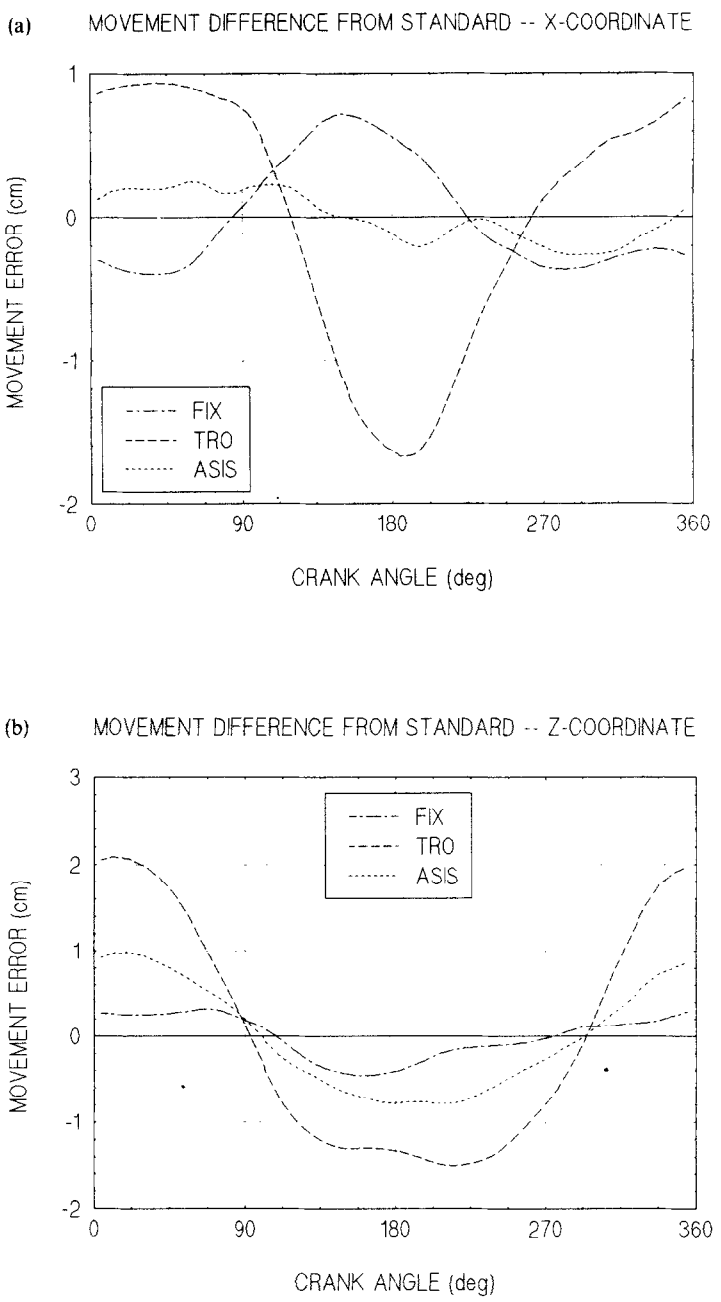

Fig. 6. Hip joint center X-coordinate (a) and Z-coordinate (b) movement difference from the standard method as a function of crank angle (90 rpm, 225 W). The movement difference was computed by subtracting the bias error associated with each method from the total error in Figs. 5(a) and (b).

Table 2. Comparison of movement error between methods (cm) (90 rpm, 225 W)

Method	Minimum value	Crank angle (deg)	Maximum value	Crank angle (deg)	Range of difference
FIX_X	−0.5	49	0.7	149	1.2
FIX_Z	−0.5	160	0.4	48	0.9
TRO_X	−1.7	186	1.0	24	2.7
TRO_Z	−1.5	216	2.1	7	3.6
$ASIS_X$	−0.3	294	0.2	64	0.5
$ASIS_Z$	−0.8	194	1.0	11	1.8

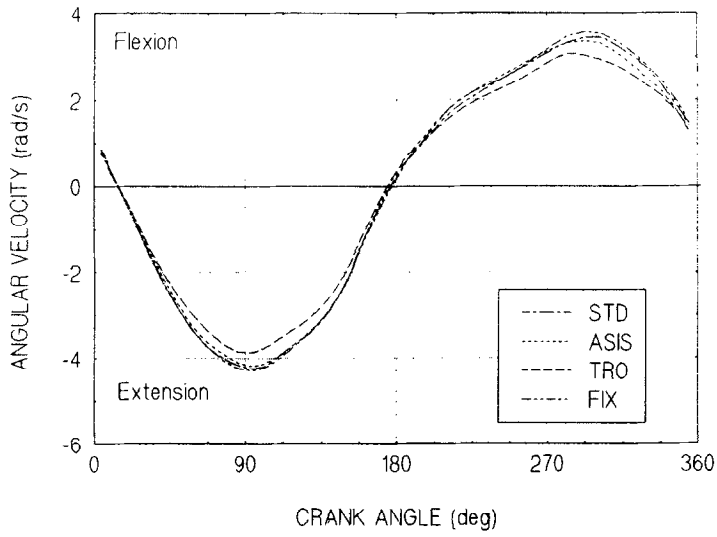

Fig. 7. Thigh angular velocity comparison as a function of crank angle (90 rpm, 225 W).

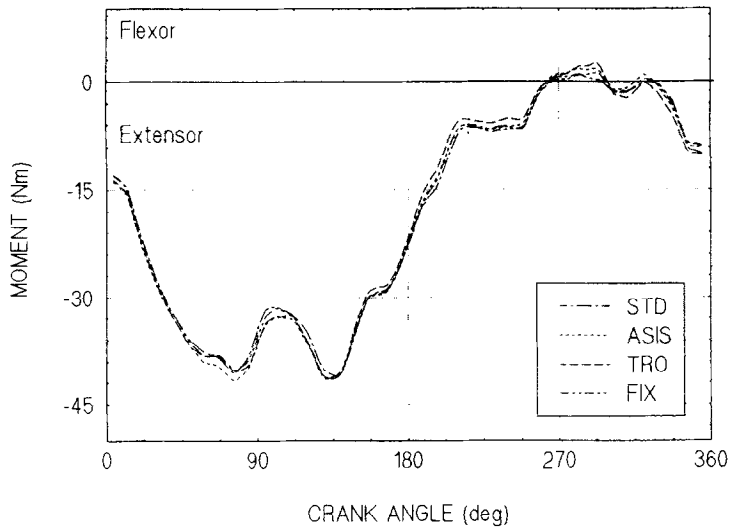

Fig. 8. Hip joint moment comparison as a function of crank angle (90 rpm, 225 W).

As mentioned in the Introduction. FIX assumes zero velocity of the hip joint resulting in zero power and work produced by the hip joint reaction force. ASIS produced peak power of 25.9 W which was 141% less error than TRO but was comparable in error to FIX. ASIS also had 184% less error in the work computation than TRO but had 100% more error than FIX. These results support the contention that ASIS leads to improved accuracy over TRO when computing biomechanical quantities of the hip. However, FIX gives better accuracy than both video based methods.

With the accuracy of ASIS determined for the pedaling rate of 90 rpm, and workrate of 225 W, the effect of pedaling rate and workrate on HJC movement and method accuracy was addressed. The results were consistent with those found for the 90 rpm, 225 W combination (Table 6). At every combination of pedaling rate and workrate, TRO had the greatest movement error while ASIS and FIX were more accurate in the X-direction, and Z-direction, respectively. Not only was ASIS consistently the most accurate in the X-direction, but it also provided the best accuracy in hip joint force power for all protocols (Table 4). However, similar to the case for 90 rpm and 225 W, the error in the hip joint force work computation was generally greater for ASIS than for FIX while TRO continued to have the greatest error for all protocols.

Using STD as the measure of hip movement, Table 7 shows that at every combination of pedaling rate and workrate, hip movement was minimum in the Z-direction at 90 rpm which is the pedaling rate most often quoted as the prefered pedaling rate of competitive cyclists (e.g. Hagberg *et al.*, 1981). Another

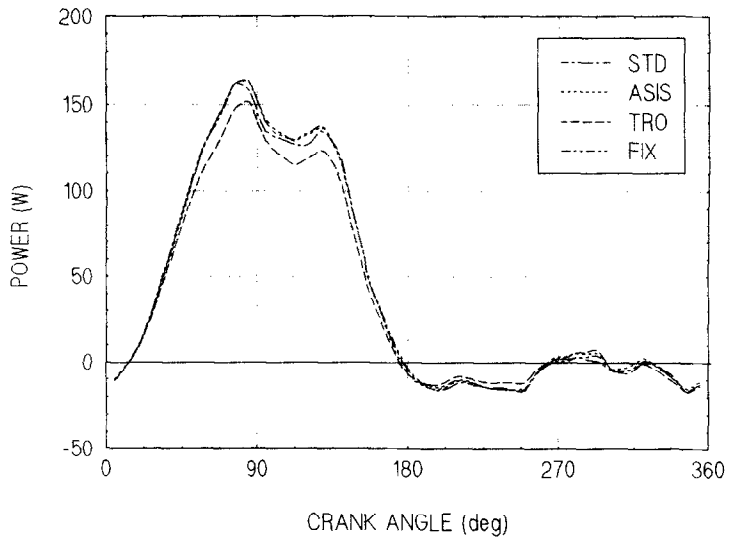

Fig. 9. Hip joint moment power comparison as a function of crank angle (90 rpm, 225 W).

Table 3. Computed hip joint moment power (W) (90 rpm, 225 W)

Method	Minimum value	Crank angle (deg)	Maximum value	Crank angle (deg)	Average value	Error of maximum (%)
STD	−22.6	243	164.4	87	38.6	—
FIX	−22.4	224	169.3	80	39.6	3.2
TRO	−19.8	253	156.3	83	35.7	4.9
ASIS	−22.4	264	169.3	79	39.6	3.0

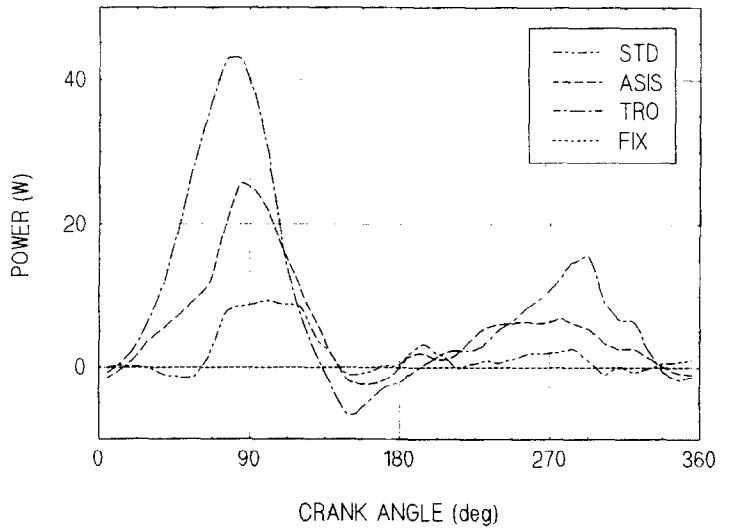

Fig. 10. Hip joint force power comparison as a function of crank angle (90 rpm, 225 W).

noteworthy result concerning hip motion is that the magnitude was minimum in the X-direction and Z-direction at the 60 rpm, 150 W and 90 rpm, 225 W combinations, respectively. Aside from these results, Tables 4, 5, and 7 indicate that there was no apparent relation between either the accuracy of hip joint force power and work computations or the magnitude of hip motion with protocol.

DISCUSSION

Because STD provides a platform for comparisons between methods, an assessment of its accuracy and limitations is warranted. Fundamental to the development of STD was the desire to eliminate the errors associated with each method under consideration. In order to avoid both soft tissue errors and marker

Table 4. Computed peak hip joint force power (W)

Pedaling rate	Workrate (W)		
	150	225	300
60 rpm			
STD	14.7	32.0	65.3
FIX	0.0	0.0	0.0
TRO	37.0	53.8	82.8
ASIS	21.4	39.0	63.9
90 rpm			
STD	8.3	12.2	39.1
FIX	0.0	0.0	0.0
TRO	29.3	43.2	71.0
ASIS	15.9	25.9	63.5
120 rpm			
STD	20.8	19.7	25.6
FIX	0.0	0.0	0.0
TRO	60.5	71.0	103.4
ASIS	33.9	38.0	47.6

Table 5. Hip joint force work as a function of pedaling rate and workrate (J)

Pedaling rate	Workrate (W)		
	150	225	300
60 rpm			
STD	4.1	9.5	15.5
FIX	0.0	0.0	0.0
TRO	15.0	26.2	39.1
ASIS	9.2	18.1	29.6
90 rpm			
STD	0.6	2.5	7.3
FIX	0.0	0.0	0.0
TRO	6.9	12.1	25.3
ASIS	3.6	7.5	20.0
120 rpm			
STD	−2.6	−1.2	0.8
FIX	0.0	0.0	0.0
TRO	1.0	3.3	14.5
ASIS	−3.4	−1.6	4.2

Table 6. Range of movement error as a function of pedaling rate and workrate (cm)

Pedaling rate	Workrate (W)		
	150	225	300
60 rpm			
FIX_X	1.2	1.5	1.7
FIX_Z	1.0	1.6	1.8
TRO_X	2.5	2.8	2.8
TRO_Z	3.3	3.6	3.8
$ASIS_X$	0.9	0.9	1.0
$ASIS_Z$	1.5	1.9	2.0
90 rpm			
FIX_X	1.5	1.3	1.9
FIX_Z	1.0	0.9	1.2
TRO_X	2.7	2.7	2.7
TRO_Z	3.4	3.6	3.8
$ASIS_X$	0.8	0.7	0.8
$ASIS_Z$	1.9	1.9	2.4
120 rpm			
FIX_X	1.5	1.6	1.4
FIX_Z	1.5	1.5	1.3
TRO_X	1.9	2.1	2.0
TRO_Z	3.9	3.6	4.1
$ASIS_X$	0.8	0.6	0.7
$ASIS_Z$	1.6	1.8	1.9

Table 7. Standard method range of movement as a function of pedaling rate and workrate (cm)

Pedaling rate	Workrate (W)		
	150	225	300
60 rpm			
STD_X	1.2	1.5	1.7
STD_Z	1.0	1.6	1.8
90 rpm			
STD_X	1.5	1.3	1.9
STD_Z	1.0	0.9	1.2
120 rpm			
STD_X	1.5	1.6	1.4
STD_Z	1.5	1.5	1.3

misalignment inherent with external markers, an invasive procedure was necessary. Due to the severity of this procedure, data were collected from only one subject. This presents an immediate limitation to the applicability of the results to the general population of cyclists. Aside from this limitation, the accuracy and integrity of the study were maintained by considering all sources of error. STD involved X-ray photography to obtain measurements of a vector locating the HJC and a coordinate transformation of this vector based on the recorded orientation of the triad coordinate system. Two possible errors became apparent during the X-ray photography. The first source was the calibration of the X-ray measurement of the vector locating the triad coordinate system origin to the HJC. To minimize this error, the precise location of the calibration device relative to the HJC was noted on the X-ray views to perform a direct linear transformation of the scaling factor used on the measurements. The second source of error was out of plane rotation of the pelvis in the lateral and anterior–posterior X-ray views. To address this error, the film axes were aligned with both the left and right anterior–superior iliac spine points through an iterative process to minimize out of plane pelvis rotation.

The accuracy of the coordinate transformation of the vector locating the HJC is dependent on the assumption that the triad coordinate system remains rigid throughout the dynamic movement of the pelvis and that the triad markers can be accurately identified. The rigidity of the triad coordinate system was investigated by an orthogonality verification between the triad axes. The results indicated that the angles between axes remained at $90 \pm 0.025°$ throughout the data acquisition. The accuracy of the marker identification was dependent on the number of cameras (3),

marker size (2.54 cm), field of view (1.0 m), and calibration and was estimated to be within 1.0 mm based on Motion Analysis Corporation system specifications.

The effect that the summation of all potential sources of error have on the accuracy of STD was addressed by an error sensitivity analysis on the measured coordinates of the vector $\mathbf{V}^{T\cdot H}$. The movement pattern of the HJC was computed with perturbations of $\pm$ 2.0 cm applied individually and in combination to each vector coordinate. The HJC range of movement was virtually unaffected by these errors with a maximum deviation of 1.6 mm from the original computations.

Data were collected for all four methods simultaneously to insure the accuracy of the comparisons between methods. This presented a possible compromise to the data if the intracortical pin interfered with the soft tissue movement in the region of the other markers. To investigate this possibility, data were collected immediately after the removal of the intracortical pin. A video marker was placed over the pin insertion point along with the anterior–superior iliac spine and trochanter markers and filmed using the standard protocol of 90 rpm and 225 W. Direct correlation analysis between the data collected with and without the intracortical pin showed that the trochanter marker movement was highly correlated at $r^2 = 0.86$ ($p = 0.0001$) in the X-direction and $r^2 = 0.98$ ($p = 0.0001$) in the Z-direction. The results of the correlation for the anterior–superior iliac spine marker were $r^2 = 0.90$ ($p = 0.0001$) and $r^2 = 0.95$ ($p = 0.0001$) in the X and Z-directions, respectively, ensuring that the intracortical pin did not inhibit the soft tissue movement.

With the accuracy of STD established, a comparison between the accuracy and errors associated with each of the three methods was conducted. TRO recorded the largest total error of the three methods. The two primary sources of this error are marker misalignment and soft tissue movement over the greater trochanter. Marker misalignment occurs when the video marker is not over the center of rotation of the HJC which produces both bias and movement errors. The bias error represents the coordinate offset from the true HJC position. Referring to Table 1, TRO had average bias errors of 0.3 and 2.3 cm in the X- and Z-directions, respectively. The bias error in the Z-direction is consistent with the anatomical position of the greater trochanter which is offset from the HJC. Marker misalignment also possibly contributes to movement errors primarily as a result of greater trochanter rotation beneath the soft tissue. This contribution might increase the range of movement error listed in Table 2 which affects the accuracy of tracking the HJC.

The other primary source of error is soft tissue movement in the greater trochanter region. With the presence of the tensor fasciae latae and gluteus medius muscle groups in this region, the magnitude of marker movement is much higher than adjacent regions of the iliac crest.

To assess the relative degree to which the marker misalignment contributed to the movement error, a post hoc experiment was performed where the trochanter marker movement was investigated with the marker in two locations. One location was the superior aspect of the greater trochanter and the other was about 3 cm above this to eliminate the bias error. Comparison of the movement patterns in these two locations indicated essentially no difference in either range of movement or phasing within a crank cycle for both coordinate directions. Because marker movement was unaffected by marker location, it follows that the soft tissue error dominated. Comparison between STD which is insensitive to this error and TRO revealed that TRO produced 2.7 and 3.6 cm more movement in the X- and Z-directions, respectively. This result emphasizes the severity of soft tissue movement errors in the greater trochanter region.

FIX is also sensitive to misalignment errors. In this case, misalignment occurs with inaccurate measurements locating the HJC relative to the reference coordinate system. The accuracy of these measurements was dependent on the relative position of the greater trochanter to the HJC. To minimize this error, repeated measurements were taken. Results from STD showed that the average coordinates for the HJC were $-$ 24.9 and 72.0 cm in the X- and Z-directions, respectively. The fixed hip measurements were recorded at -25.0 and 71.0 cm resulting in an error of 1 cm in the Z-coordinate direction. But even if this error could be eliminated by methods which accurately locate the HJC position, the primary limitation to FIX is the assumption that the HJC remains stationary. This study showed that actual hip movement for 90 rpm at 225 W exceeded 1.3 and 0.9 cm in the X- and Z-directions, respectively which were close to the minimum values for all combinations of pedaling and workrates. HJC movement of this magnitude yields evidence that FIX is prone to error.

ASIS was introduced to minimize errors inherent with TRO and FIX. The goal was to reduce movement errors arising from both soft tissue and marker misalignment while maintaining the dynamic integrity of the HJC movement. Although using a video marker over the anterior–superior iliac spine reduced movement errors due to the above sources, other possible errors are introduced. First, ASIS assumes no rotation of the pelvis in the sagittal plane by using a fixed vector in both orientation and magnitude to locate the HJC from the anterior–superior iliac spine. Data from the triad markers showed the pelvis rotation in the sagittal plane to be less than 3° validating this assumption for the subject used herein.

Establishing the vector from the anterior–superior iliac spine to the HJC is also prone to error. The vector was established by computing the average distances in the X- and Z-directions between the anterior–superior iliac spine and trochanter markers

using video analysis. Errors are introduced by the bias error associated with the trochanter marker. Referring to Table 1, the mean offsets for the trochanter data were 0.3 and 2.3 cm in the X- and Z-directions, respectively, which also correspond to the bias errors of ASIS. However, in contrast to TRO, the bias error does not lead to any movement error since the anterior–superior iliac spine marker is attached to the skin over a bony prominence of the pelvis and the vector locating the trochanter is spatially fixed.

As a consequence of errors in HJC movement introduced by the three methods, computed biomechanical quantities were also prone to error. The amount of trochanter movement in the Z coordinate reported here is similar in magnitude to Gregor *et al.* (1991) who measured hip movement in the vertical direction up to 3 cm. They concluded that hip motion of this magnitude can affect hip joint moment calculations by 5–10%. This conclusion is consistent with the results of this study. The hip joint moment produced by TRO varied by as much as 9% from the results from STD.

Hip movement errors introduced by TRO have a greatest relative impact on hip joint force power and work calculations. van Ingen Schenau *et al.* (1990) used TRO to compute a maximum power exceeding 70 W while cycling at 90 rpm and 350 W. The subject of this study produced a maximum power of 71 W at 90 rpm and 300 W which is consistent with van Ingen Schenau *et al.* (1990). At this pedaling rate and workrate, STD produced 39 W resulting in an over estimate of 32 W or 80% error. This over estimate existed throughout the crank cycle (Fig. 10) which directly affected the calculation of mechanical energy expenditure (MEE) by overestimating the work fraction developed by this source (Aleshinsky, 1986a, b). Integrating the instantaneous power curve over the crank cycle over estimated the work produced by the joint force by 18 J (Table 5). In fact for all combinations of pedaling rate and workrate, TRO consistently led to over estimates of hip joint force work which averaged more than four times that produced by STD.

The effect of the error introduced by FIX also became apparent when computing biomechanical quantities. By assuming zero velocity at the HJC, any power developed by the hip joint force is eliminated. As previously discussed, the consequence of this result is that inaccuracy is introduced into calculations of MEE.

Although FIX is prone to these errors, FIX is not entirely without utility. The accuracy of FIX is dependent on the hip movement of the individual cyclist. The results of this study indicate that the hip movement was minimum at the 60 rpm, 150 W and 90 rpm, 225 W combinations which minimize the errors associated with FIX. A comparison of the work produced by the hip joint force with ASIS and TRO at 90 rpm and 225 W indicates that FIX is more accurate. Table 5 indicates that assuming zero work developed by the joint force (i.e. assuming a fixed hip) is generally more accurate for the various combinations of pedaling rate and workrate because of the large overestimates produced by the two video methods. It should be noted that the work computation errors associated with FIX were maximized at the higher workrates as a result of increased power produced by the hip joint.

The results of the peak hip joint force power computations for all combinations of workrate and pedaling rate were unintuitive based on the work calculations. Table 4 indicates that the 90 rpm and 225 W combination was the only protocol where FIX was more accurate than ASIS. TRO had the highest error averaged over all combinations at 177%. This indicates that ASIS is more accurate in computing instantaneous power produced by the hip joint force.

CONCLUSIONS

The main conclusions of this paper are twofold. First, ASIS indicated the movement of the HJC with less error than TRO. A comparison with STD illustrated the increase in accuracy of computed biomechanical quantities due to this decrease in error. Second, the magnitude of hip motion measured by STD established that FIX is prone to error. Therefore FIX introduced error into computed biomechanical quantities by ignoring the dynamic movement of the HJC. For the subject of this study, the magnitude of the instantaneous power developed by the hip joint force was substantial for most protocols and was computed more accurately using ASIS. But comparisons between methods showed that FIX was the most accurate over all workrates and pedaling rates when computing hip joint work produced over the crank cycle which improves the accuracy of mechanical energy expenditure calculations. These results suggest that the method used to track the HJC in cycling research should depend on the biomechanical quantities of interest.

Acknowledgements—We are thankful to Shimano Corporation of Osaka, Japan for their continued financial support of this research. We also want to express our appreciation to both Dr Stephen Howell for performing the surgical procedures and Dwight Morejohn for rendering Fig. 2.

REFERENCES

Aleshinsky, S. Y. (1986a) An energy 'sources' and 'fractions' approach to the mechanical energy expenditure problem—I. Basic concepts, description of the model, analysis of a one-link system movement. *J. Biomechanics* **19**, 287–293.

Aleshinsky, S. Y. (1986b) An energy 'sources' and 'fractions approach to the mechnical energy expenditure problem–II. Movement of the multi-link chain model. *J. Biomechanics* **19**, 295–300.

Gregor, R. J., Broker, J. P., Ryan and M. M. (1991) The biomechanics of cycling. *Exer. Sport Sci. Rev.* **19**, 127–169.

Gregor, R. J., Cavanagh, P. R. and LaFortune, M. (1985) Knee flexor moments during propulsion in cylcing—A

creative solution to Lombard's paradox. *J. Biomechanics* **18,** 307–316.

Hagberg, J. M., Mullin, J. P., Giese, M. D. and Spitznagel, E. (1981) Effect of pedaling rate on submaximal exercise responses of competitive cyclists. *J. Appl. Physiol.* **51,** 447–451.

Hull, M. L. and Gonzalez, H. K. (1990) The effect of pedal platform height on cycling biomechanics. *Int. J. Sports Biomech.* **6,** 1–17.

Hull, M. L. and Jorge, M. (1985) A method for biomechanical analysis of bicycle pedaling. *J. Biomechanics* **18,** 631–644.

Newmiller, J., Hull, M. L. and Zajac, F. E. (1988) A mechanically decoupled two force component bicycle pedal dynamometer. *J. Biomechanics* **21,** 375–386.

van Ingen Schenau, G. J., van Woensel, W. W. L. M., Boots, P. S. M., Snackers, R. W. and deGroot, G. (1990) Determination and interpretation of mechanical power in human movement: application to ergometer cycling. *Eur. J. Appl. Physiol.* **61,** 11–19.

APPENDIX

To compute the hip joint center (HJC) position using the standard method (STD), Cartesian coordinate systems were established in the laboratory (X, Y, Z) and triad markers (x, y, z) (Fig. 2). The bases for each of the coordinate systems are denoted by the unit vectors $\hat{\mathbf{I}}, \hat{\mathbf{J}}, \hat{\mathbf{K}}$, (laboratory) and $\hat{\mathbf{i}}, \hat{\mathbf{j}}, \hat{\mathbf{k}}$ (triad markers). The origin of the laboratory coordinate system was located along the crank spindle axis at the point where the axis intersects the outside surface of the right crank arm. The X-axis was directed horizontally towards the front of the bicycle, the Y-axis parallel to the crank spindle, and the Z-axis mutually perpendicular. The origin of the triad coordinate system was located at the triad center T_C. The directions of the triad axes were determined by the triad markers. The x-axis was directed anteriorly parallel to the line joining markers T_2 and T_3, the y-axis medially along the axis of the pin, and the z-axis superiorly along the line joining points T_m and marker T_1.

The location of the HJC in the laboratory coordinate system was computed in three steps. First, the fixed vector $\mathbf{V}^{TrH} = v_1\hat{\mathbf{I}} + v_2\hat{\mathbf{J}} + v_3\hat{\mathbf{K}}$ measured from the X-ray views in the laboratory system was transformed into a triad fixed coordinate system by a direction cosine transformation. Direction cosines were derived by first expressing vectors defining the triad fixed coordinate system as

$$\mathbf{x} = x_1\hat{\mathbf{I}} + x_2\hat{\mathbf{J}} + x_3\hat{\mathbf{K}}, \quad \mathbf{y} = y_1\hat{\mathbf{I}} + y_2\hat{\mathbf{J}} + y_3\hat{\mathbf{K}}, \quad \mathbf{z} = z_1\hat{\mathbf{I}} + z_2\hat{\mathbf{J}} + z_3\hat{\mathbf{K}}. \tag{A1}$$

The components of the triad axes defined in terms of the spherical markers were:

$$\begin{aligned} x_1 &= T_{3X} - T_{2X}, \quad y_1 = T_{pX} - T_{cX}, \quad z_1 = T_{1X} - T_{mX}, \\ x_2 &= T_{3Y} - T_{2Y}, \quad y_2 = T_{pY} - T_{cY}, \quad z_2 = T_{1Y} - T_{mY}, \\ x_3 &= T_{3Z} - T_{2Z}, \quad y_3 = T_{pZ} - T_{cZ}, \quad z_3 = T_{1Z} - T_{mZ}. \end{aligned} \tag{A2}$$

The unit vectors of the triad axes became

$$\hat{\mathbf{i}} = \frac{\mathbf{x}}{|\mathbf{x}|}, \quad \hat{\mathbf{j}} = \frac{\mathbf{y}}{|\mathbf{y}|}, \quad \hat{\mathbf{k}} = \frac{\mathbf{z}}{|\mathbf{z}|}, \tag{A3}$$

resulting in the final direction cosines:

$$\begin{aligned} &\cos\theta_{Xx} = \hat{\mathbf{I}}\cdot\hat{\mathbf{i}} = \frac{x_1}{|\mathbf{x}|}, \quad \cos\theta_{Yx} = \hat{\mathbf{J}}\cdot\hat{\mathbf{i}} = \frac{x_2}{|\mathbf{x}|}, \quad \cos\theta_{Zx} = \hat{\mathbf{K}}\cdot\hat{\mathbf{i}} = \frac{x_3}{|\mathbf{x}|}, \\ &\cos\theta_{Xy} = \hat{\mathbf{I}}\cdot\hat{\mathbf{j}} = \frac{y_1}{|\mathbf{y}|}, \quad \cos\theta_{Yy} = \hat{\mathbf{J}}\cdot\hat{\mathbf{j}} = \frac{y_2}{|\mathbf{y}|}, \quad \cos\theta_{Zy} = \hat{\mathbf{K}}\cdot\hat{\mathbf{j}} = \frac{y_3}{|\mathbf{y}|}, \\ &\cos\theta_{Xz} = \hat{\mathbf{I}}\cdot\hat{\mathbf{k}} = \frac{z_1}{|\mathbf{z}|}, \quad \cos\theta_{Yz} = \hat{\mathbf{J}}\cdot\hat{\mathbf{k}} = \frac{z_2}{|\mathbf{z}|}, \quad \cos\theta_{Zz} = \hat{\mathbf{K}}\cdot\hat{\mathbf{k}} = \frac{z_3}{|\mathbf{z}|}. \end{aligned} \tag{A4}$$

To transform from the $\hat{\mathbf{I}}, \hat{\mathbf{J}}, \hat{\mathbf{K}}$ basis to the $\hat{\mathbf{i}}, \hat{\mathbf{j}}, \hat{\mathbf{k}}$ basis, the resulting form of the direction cosine matrix is

$$M = \begin{bmatrix} \cos\theta_{Xx} & \cos\theta_{Yx} & \cos\theta_{Zx} \\ \cos\theta_{Xy} & \cos\theta_{Yy} & \cos\theta_{Zy} \\ \cos\theta_{Xz} & \cos\theta_{Yz} & \cos\theta_{Zz} \end{bmatrix} \tag{A5}$$

yielding the transformed vector $\mathbf{V}^{TrH'}$ expressed in the triad fixed coordinate system as

$$\mathbf{V}^{TrH'} = v_1'\hat{\mathbf{i}} + v_2'\hat{\mathbf{j}} + v_3'\hat{\mathbf{k}}, \quad \begin{aligned} v_1' &= \cos\theta_{Xx}v_1 + \cos\theta_{Yx}v_2 + \cos\theta_{Zx}v_3, \\ v_2' &= \cos\theta_{Xy}v_1 + \cos\theta_{Yy}v_2 + \cos\theta_{Zy}v_3, \\ v_3' &= \cos\theta_{Xz}v_1 + \cos\theta_{Yz}v_2 + \cos\theta_{Zz}v_3. \end{aligned} \tag{A6}$$

The fixed vector $\mathbf{V}^{TrH'}$ established the HJC relative to the pin marker T_p in the triad fixed coordinate system.

Next, a direction cosine transformation of vector $\mathbf{V}^{TrH'}$ back into the laboratory reference system as a function of time was performed. The direction cosine matrix was the transpose of the matrix above. This transformation yielded the vector $\mathbf{V}^{TrH''}$ expressed in the laboratory coordinate system as

$$\mathbf{V}^{TrH''} = v_1''\hat{\mathbf{I}} + v_2''\hat{\mathbf{J}} + v_3''\hat{\mathbf{K}}, \quad \begin{aligned} v_1'' &= \cos\theta_{Xx}v_1' + \cos\theta_{Xy}v_2' + \cos\theta_{Xz}v_3', \\ v_2'' &= \cos\theta_{Yx}v_1' + \cos\theta_{Yy}v_2' + \cos\theta_{Yz}v_3', \\ v_3'' &= \cos\theta_{Zx}v_1' + \cos\theta_{Zy}v_2' + \cos\theta_{Zz}v_3'. \end{aligned} \tag{A7}$$

The final step located the HJC by vector addition. The pin marker vector $\mathbf{V}^{LcTr} = p_1\hat{\mathbf{I}} + p_2\hat{\mathbf{J}} + p_3\hat{\mathbf{K}}$ recorded with video analysis in the laboratory coordinate system was added to the triad vector $\mathbf{V}^{TrH''}$ computed in equation (A7). Vector addition yielded the three dimensional HJC coordinates in the laboratory system as

$$\mathbf{V}^{LcH} = \mathbf{V}^{LcTr} + \mathbf{V}^{TrH''} = (p_1 + v_1'')\hat{\mathbf{I}} + (p_2 + v_2'')\hat{\mathbf{J}} + (p_3 + v_3'')\hat{\mathbf{K}}. \tag{A8}$$